

# Morphological, Rheological and Ultrasonic Characterizations of ECO-Friendly Microemulsion Lattices Based on Acrylate Monomers.

H. E. Nasr<sup>1\*</sup>, M.S. Gaafar<sup>2</sup>, O. Abdel-Kareem<sup>3</sup> and F. Abd El-Aziz<sup>4</sup>

<sup>1</sup>Department of Polymers and Pigments National Research Centre, Cairo, Egypt

<sup>2</sup>Ultrasonic Department National Institute for Standards El Harem, Giza, Egypt

<sup>3</sup>Conservation Department, Faculty of Archaeology, Cairo University

<sup>4</sup>Engineering and Surface Metrology Department, National Institute for Standards El Harem, Giza, Egypt

\*[hanaa\\_nasr@hotmail.com](mailto:hanaa_nasr@hotmail.com)

**Abstract:** In this work microemulsion copolymers having different composition ratios of methyl methacrylate (MMA) and hydroxyethyl methacrylate (HEMA) were prepared using ultrasonic initiation system in presence of sodium lauryl sulphate (SLS) as an emulsifier. The obtained copolymers were characterized using FTIR, morphological and particle size analysis using atomic force microscope (AFM), differential scanning calorimetry, (DSC), X-ray analysis and rheological properties. The results showed that the prepared microemulsion lattices having nano-sized diameter ranged between 40-115 nm. Increasing HEMA content in the feed comonomer composition (0-25%) was accompanied by increasing particle size diameter and solution viscosities while, the glass transition temperature was decreased. Ultrasonic wave propagation has been studied using pulse-echo method at a frequency of 2 MHz. The ultrasonic velocities (longitudinal & transverse) and density have been used to calculate the elastic moduli at different concentrations. The ultrasonic absorption coefficient has been also measured. Various ultrasonic parameters have been computed from the experimental values. The variations of ultrasonic absorption coefficient, adiabatic compressibility, acoustic impedance and free length show that these parameters affected with monomer feed compositions but the variation is slightly non-linear. Ultrasonic viscosity values of the prepared microemulsion latex have been determined and the obtained data was compared with that obtained using coaxial-cylinder method. [Journal of American Science 2010; 6(9):897-910]. (ISSN: 1545-1003).

**Key words:** Microemulsion; AFM, rheological, DSC, ultrasonic velocities; ultrasonic attenuation coefficient; ultrasonic viscosity

## 1. Introduction:

Many authors proved that ultrasonic irradiation is considered as a novel technique to synthesize ultraclean polymer particles<sup>[1-3]</sup>. This technique showed many advantages such as the absence of a chemical initiator, fast polymerization rates, and polymers of high molecular weight with narrow size distribution<sup>[1]</sup>. In emulsion polymerization, ultrasonic is used to prepare different homopolymer and copolymers of different monomers<sup>[4]</sup>. Wang et al<sup>[5]</sup> synthesized polystyrene using ultrasonic irradiation of power 20 khz and the obtained polymer was of particle size about 30nm. Also, Lifeng Yan et al<sup>[6]</sup> prepared in a surfactant-free aqueous emulsion copolymer of styrene/acrylamide using ultrasonic irradiation of power 20 khz. The molecular weight of the obtained copolymer is  $1.86 \times 10^5$  and the polydispersity index is 2.31. Miniemulsion polymer having smaller particle size than emulsion polymer could be also prepared using ultrasonic irradiation<sup>[1,7&8]</sup> in presence of little amounts of chemical initiation; the extension of this work, microemulsion polymerization can be used to prepare nanosized particles by the application of ultrasonic. Teo et al<sup>[9]</sup> prepared nanosized polymer latex

particles using high-frequency ultrasound (213 kHz). They studied the effects of surfactant type and concentration of surfactants on the rates of polymerization, latex size, and molecular weights of the polymers. The microemulsion (ME) and conventional emulsion (CE) copolymerizations of methyl methacrylate (MMA) with acrylonitrile (AN) are carried out<sup>[10]</sup> at 70°C by employing *n*-butyl cellosolve as cosurfactant along with sodium lauryl sulfate as surfactant in the reaction medium and potassium persulphate as initiator. The copolymers are characterized by FTIR, NMR, TG/DTA, and GPC techniques. Characterization of polymeric materials has been carried out by means of thermodynamic, mechanical and spectroscopic methods. The ultrasonic velocity and the elastic properties are of the most important factors determining the polymers properties; several experimental methods have been used to estimate the static and dynamic viscoelastic properties. Further parameters such as ultrasonic absorption, ultrasonic viscosity, adiabatic compressibility, acoustic impedance and Rao's constant can be calculated. These parameters are useful in understanding the nature of interactions of

polymers. Several earlier papers have addressed these problems for polymers in single solution<sup>[11-14]</sup>.

This work aimed to study the characteristic behaviors of microemulsion lattices prepared from MMA and MMA/HEMA (having different monomers composition ratios) using Eco-friendly initiation system represented as ultrasonic mechanism. The characterization involves measurements of morphology (using AFM); FT-IR; thermal analysis (TGA & DSC), X-ray diffraction and flow behaviour. Moreover, different ultrasonic parameters were performed for the prepared microemulsion latex to study the effect of different feed monomer composition as well as SLS concentrations of the microemulsion on such parameters.

## 2. Experimental

### Chemicals

Methyl methacrylate (MMA) and Hydroxy ethyl methacrylate (HEMA) monomers were supplied

by Merck-Schuchardt, Germany and redistilled before use. The purified monomer was sealed and stored below 4 °C until further use. Sodium lauryl sulphate (SLS) was product of the BDH, Australia. Distilled water was used as the polymerization medium.

### Polymerization procedure

The polymerization reactions were carried out with a total sample volume of 100 ml, Specific amount of purified monomers (MMA & HEMA) (8gm), surfactant (SLS) (2&5 gm) and desired amount of distilled water (to complete the reaction volume 100ml), were introduced into the reaction vessel conducted with circulated water to maintain the desired temperature. Then the ultrasonic generator (Branson Sonifier S-450 A, USA) was switched on and the reaction was subjected to ultrasonic irradiation. After a certain time of the reaction, ultrasonic irradiation was stopped. The power input was adjusted to be 0.1 W/ml.

**Table (1): Recipe of microemulsion polymerization of different composition ratios MMA/HEMA at constant ultrasonic irradiation**

Sample code	Feed monomer composition ratio (%)	Amount of surfactant (gm)	Average particle diameter $D_v$ (nm)
Polymer I	MMA (100)	2	68
Copolymer II	MMA/HEMA (93.75/6.25)	2	88
Copolymer III	MMA/HEMA (87.5/12.5)	2	118
Copolymer IV	MMA/HEMA (81.75/18.25)	2	129
Copolymer V	MMA/HEMA (75/25)	2	140
Polymer VI	MMA (100)	5	--
Copolymer VII	MMA/HEMA (93.75/6.25)	5	--
Copolymer VIII	MMA/HEMA (87.5/12.5)	5	--

### Characterization

FT-IR spectroscopy was carried out using Nicolet 380, Thermo FTIR spectrophotometer. Average particle size of the obtained microemulsion was determined by Atomic Force Microscope AFM on JEM 100 CX/2 instrument (JEOL Co, Japan). The Thermogravimetric (TG) and The Differential scanning calorimetric (DSC) measurements for the obtained microemulsion samples were carried out at a temperature range starting from 50°C to 700°C under nitrogen atmosphere with heating rate of 10°C/min using Shimadzu TGA-50 and Shimadzu DSC -50, Japan. X-ray diffraction for the prepared samples was investigated by x-ray diffraction by using Philips analytical X-ray B.V. The flow behavior of all the examined samples were measured at shear rate range

of (500-1400 sec<sup>-1</sup>) at 25°C ±1°C, using Bohlin rheometer model CS10, UK. The samples were measured using Cone Plate (CP 4°/40mm).

### Ultrasonic measurements procedure

The ultrasonic velocities in the liquid mixtures were measured using pulse-echo method operating at a frequency of 2MHz (central frequency of 0.7 MHz and bandwidth of 1.4 MHz). The uncertainty of the measurements is 10 m/sec. Using an oscilloscope (60 MHz time base oscilloscope, Philips, Netherlands) direct measurement of the time required for the pulses to travel twice the length of the specimen is possible, to allow immediate calculation of the ultrasonic wave velocity as given in the following equation:

$$v = \frac{2L}{\Delta t} \quad (1)$$

Where L is the liquid length and  $\Delta t$  is the time interval.

The ultrasonic absorption coefficient ( $\alpha$ ) and ultrasonic viscosity ( $\eta_u$ ) are given in the form;

$$\alpha = \frac{20}{2L} \log (A_n / A_{n+1}) \quad (2)$$

$$\eta = \frac{\rho \alpha v^3}{26.3f^2} \quad (3)$$

Where  $A_n / A_{n+1}$  is the ratio between two successive echoes  $A_n$ ,  $A_{n+1}$ ,  $\rho$  is the density of the oil and  $f$  is the ultrasonic frequency. The uncertainty of the measurements of ultrasonic absorption and viscosity are  $\pm 0.01$  dB/cm and  $\pm 0.03$  mPa.s respectively. The experimental measurements were performed for all examined microemulsion samples having varied densities at ambient temperature  $25^\circ \pm 2^\circ\text{C}$ . Each experiment was repeated three times and through three days consecutively, and the median was chosen as an end result

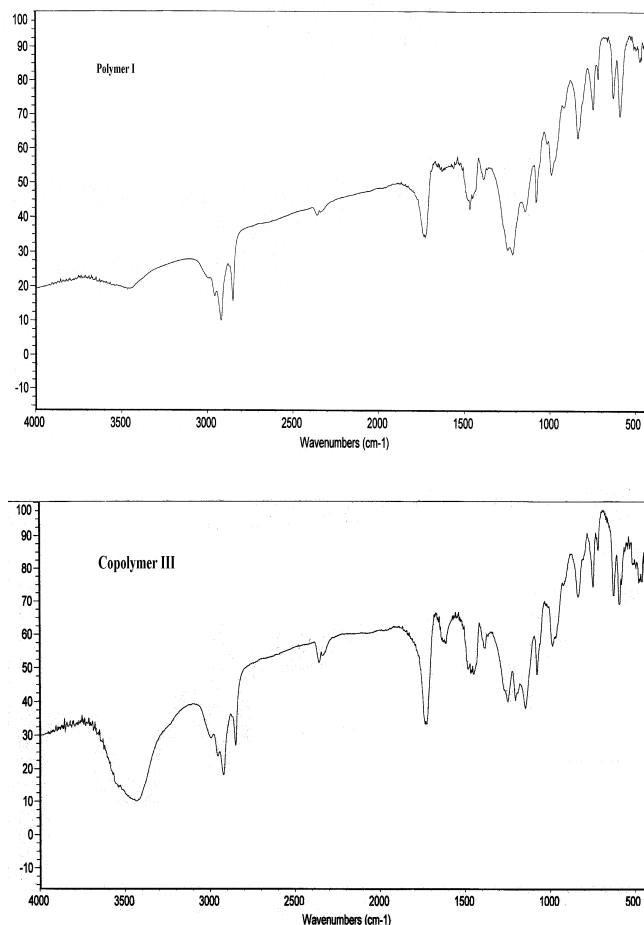
### 3. Results and Discussion: FTIR

Figure (1 a & b) illustrates the FTIR spectra of polymer I and copolymer III. It is seen that, for both illustration there are characteristic bands at  $1731\text{ cm}^{-1}$  for C=O,  $2950\text{ cm}^{-1}$  for C-H stretching bands which confirm presence of PMMA chains. The presence of broad band at approximately  $3300\text{-}3500\text{ cm}^{-1}$  characteristic for OH groups only in Figure 1b is an indication for presence of HEMA in the copolymer.

#### Morphological characterization

Morphological characterization of the obtained microemulsion samples, prepared at different monomers composition ratios, by AFM is shown in Figure 2. The corresponding average particle diameters are listed in Table 1. It is evident that the average particle diameter increases by increasing the content of HEMA in feed monomer composition. The particle diameter for poly MMA was 68 nm and increased by increasing HEAMA contents to reach 129 and 140 nm for polymer IV & V respectively. These results agree with the former results showed by Pişkin<sup>[15]</sup> and Bhawal<sup>[16]</sup> and this behavior is a direct result of the difference in the monomer partitioning of MMA and HEMA in the different phases involved in the particle formation and the subsequent

stabilization of the particles by the available surfactant.



**Figure (1): FTIR spectra of PMMA and copolymer III**

#### X- ray Diffraction analysis

The effect of the HEMA content on the crystallization of PMMA I and copolymers II-VIII could also be confirmed from the results of X-ray diffraction in Figure (3). One peak was found for either PMMA or copolymers II-VIII. This peak at  $2\theta = 20^\circ$  and it has high intensity. With increasing the content of HEMA in the copolymers II-VIII, the relative intensity of the peak decreases significantly. In general, a polymer with crystalline region will have sharp X-ray diffraction peaks with high intensities, whereas the X-ray diffraction peaks will be broad for an amorphous polymer<sup>[17]</sup>. As HEMA is an amorphous polymer, the existence of HEMA in the copolymers I-VIII reduced the percentage of PMMA in the copolymer and resulted in the decrease of peak intensity.

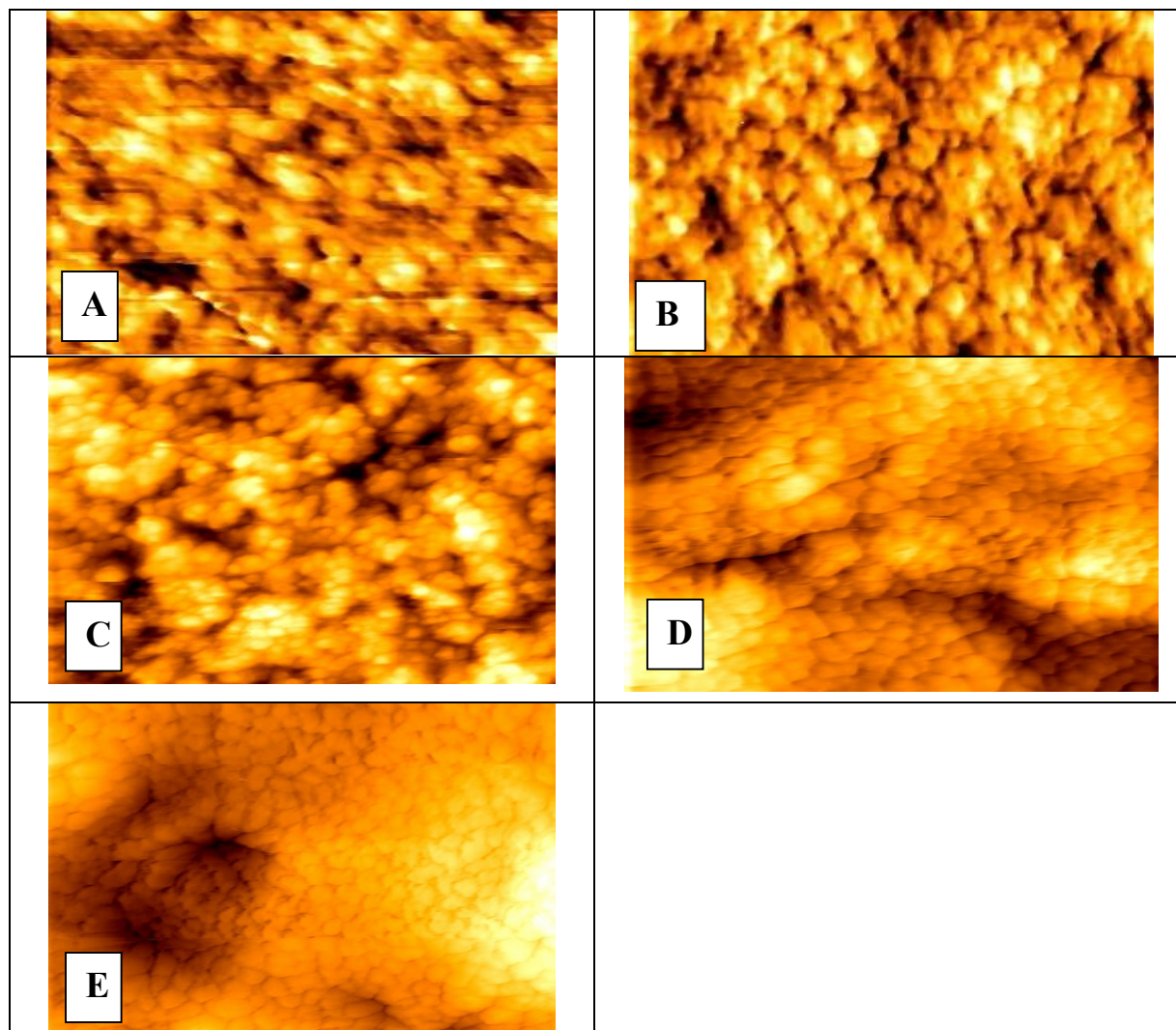


**Figure (2): AFM for (A) PMMA, (B) copolymer II, (C) copolymer III, (D) copolymer IV and (E) copolymer V**

#### Thermal properties

##### Thermogravimetric analysis (TGA)

Figure (4) shows the TG/DrTGA curves of polymer I, IV and V. It is evident that the thermal degradation of pure PMMA has three distinctive steps. The first step starts at temperature of ( $T_i$ ) 190°C and ends ( $T_f$ ) at 270°C with decomposition temperature ( $T_d$ ) of 240°C. The second step has  $T_i$ ,  $T_f$  and  $T_d$  values of 360, 398 and 382°C, respectively. The third step of thermal degradation is over 400°C. The three thermal degradation steps of polymer I are due to the unzipping from the head to head linkage, the vinylidene chain end and random loci of the methacrylate chain, respectively [18]. On the other hand, the TG/DrTGA curves copolymer IV and V show two main differences from polymer I. Firstly, appearances of new degradation step at temperature range from 180 to 202°C which could be related to

the presence of HEMA unit in the molecular structure of the copolymer. Secondly, there is lowering in the initiation decomposition temperature of the vinylidene chain end step by about 14 and 22°C for the two copolymers, respectively. As a result, it could be concluded that the incorporation of HEMA into the PMMA chains reduces the thermal stability of PMMA significantly.

##### Differential scanning calorimetry (DSC)

Figure (5) shows the DSC curves for each of copolymers I-V as well as SLS. It is seen that all of studied samples showed nearly similar DSC curves. Also, there is a small endothermic peak in the traces of both the copolymers at 76°C. This peak may be related to the glassy transitions for the copolymers. There is another endothermic peak at 115°C that appeared for the DSC curves of pure SLS and the

copolymers I-VIII, which may be attributed to the crystallization of pure SLS and the copolymers I-VIII. Another endothermic duplicate peak in the range of 181–187°C appeared for the DSC curve of pure SLS and the copolymers I-VIII. This peak was shifted to lower temperature depending on the percentage content of HEMA in the copolymer, which may be attributed to the start of melting. An

endothermic peak around 264.5°C may be due to the oxidation of SLS. Starting of the oxidation for copolymers I-VIII is also around 390°C, and it is completed around 460°C. The DSC analysis also suggests that the copolymers I-VIII are thermally less stable with addition of HEMA in the copolymer, which means the increase in the chain mobility.

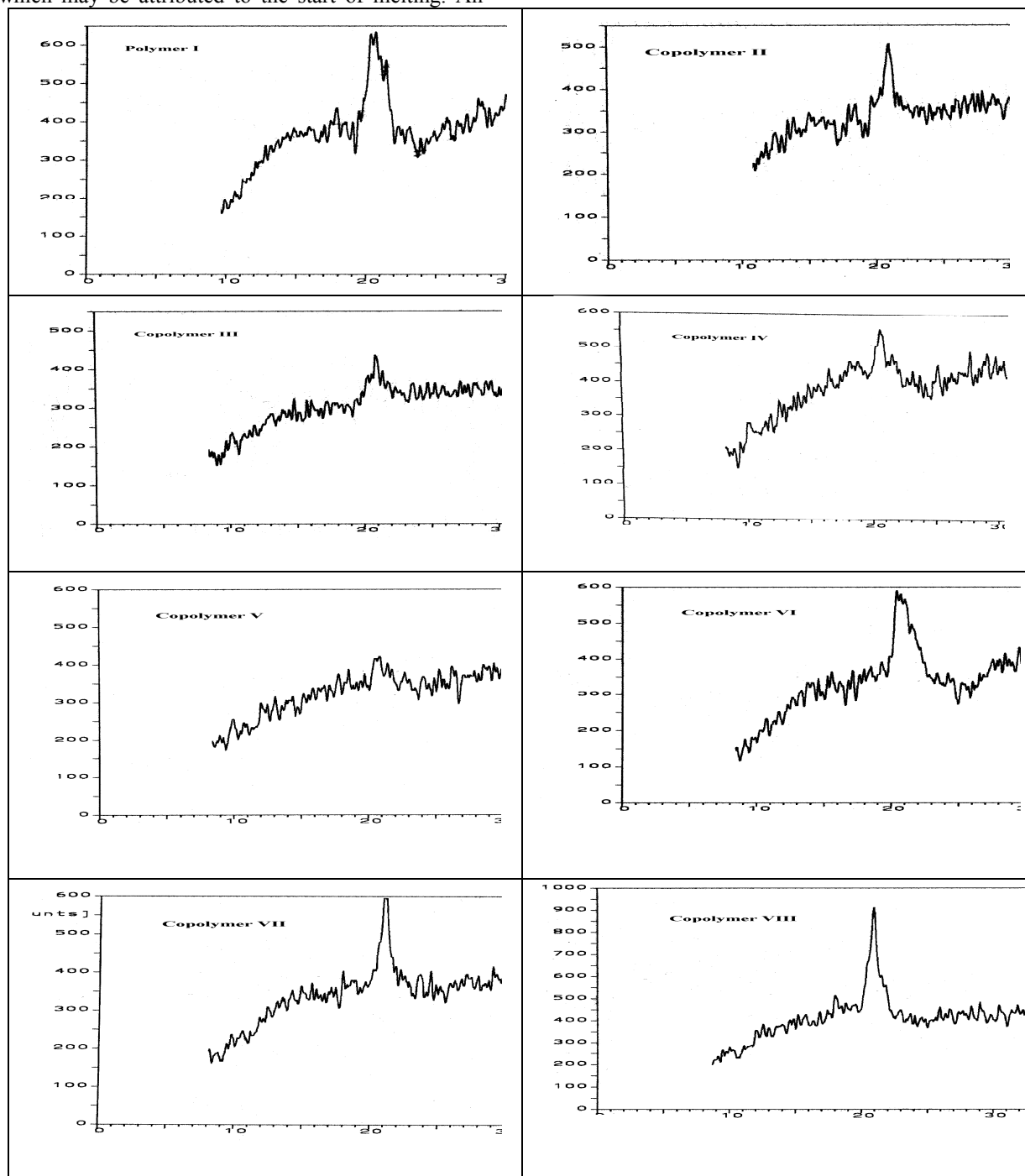


Figure (3): X-ray diffraction patterns of PMMA and MMA/HEMA copolymers having different composition ratios.

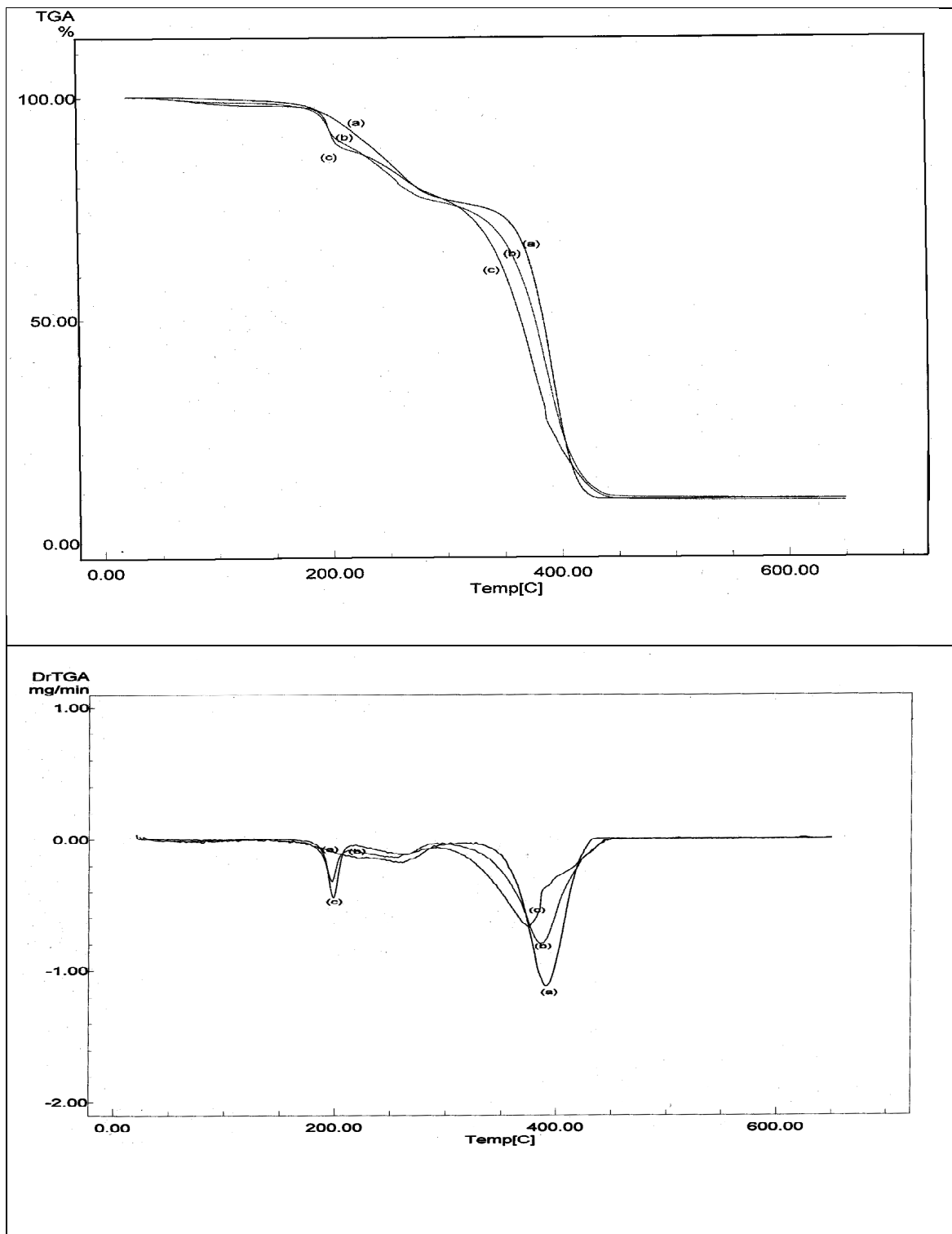


Figure (4): TGA/DrTGA thermograms of (a) PMMA, (b) copolymer IV and (c) copolymer V.

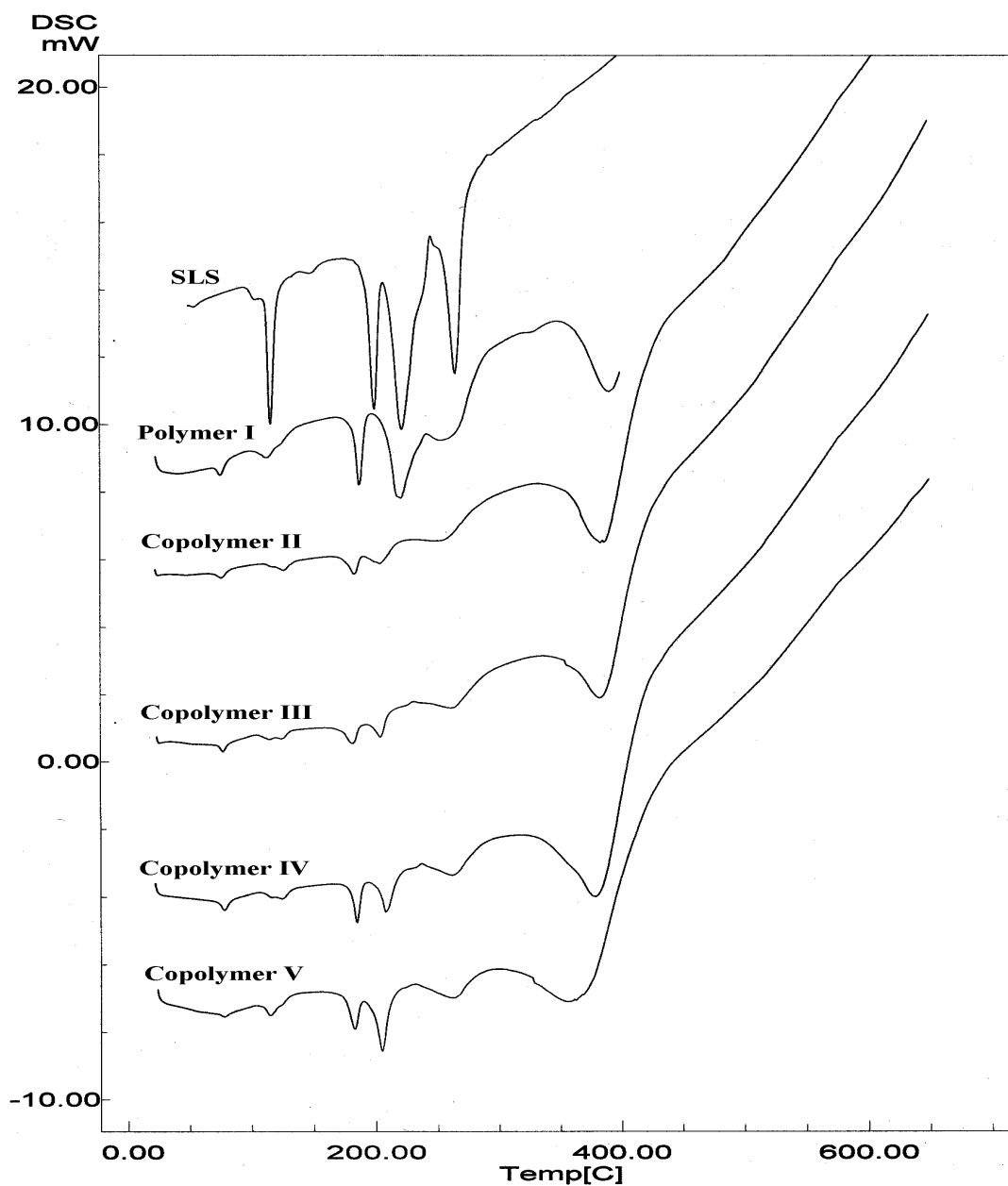


Figure (5): DSC curves for SLS and MMA/BuA copolymers having different composition ratios.

#### Ultrasonic properties

Figure 6 (a, b) shows the variation of ultrasonic velocity with HEMA % in the feed monomer composition of the copolymer microemulsion samples. It is evident that the values of ultrasonic velocity increase with increasing the weight percentage of HEMA. In general, the increase of ultrasonic wave velocity is related to the decrease in inter-molecular spacing of the material<sup>[19]</sup>. The change of ultrasonic velocity as a result of the good interaction throughout the entire composition range due to the chemical reactions between the

constituents, and this has been confirmed by the occurrence of single glass transition temperature for all the compositions studied<sup>[20]</sup>. The rate of increase of ultrasonic velocity in the copolymers with higher SLS content (5%) was found to be higher than the rate in the copolymers with less SLS content (2%). These results may be correlated to two reasons; a) the association of the emulsifier molecules when their concentration exceeds the critical micelle concentration (CMC)<sup>[21–24]</sup>, b) this rate increase in ultrasonic velocity can be explained by the decrease in free length  $L_f$  (i.e. the decrease in the distances

between molecular surfaces) as can be seen in Tables (2 & 3).

Young's modulus (E) and microhardness (H) are increased from 1.38 to 1.8 GPa and 0.046 to 0.080 GPa, respectively, as the percentage ratio of HEMA (polymer) increases from 0 to 25 % in the feed monomer composition. On the other hand, the rate of increasing of Young's modulus and microhardness is more observed when the HEMA content increases to about 5%, Table 3. Their values were found to increase from 1.35 to 1.76 GPa and 0.044 to 0.079 GPa, respectively. The increase of (E) and (H) in both cases was suggested to the decrease in free length  $L_f$ , which means the association (aggregation) of emulsifier molecules. The higher rate of increasing in (E) and (H) when the emulsifier (SLS) is increased was due to the association of the emulsifier molecules when their concentration exceeds the critical micelle concentration (CMC) [21-24].

The ultrasonic absorption coefficient of the studied microemulsion samples was measured and the results are listed in Table 3. In spite of some scatters of the measured values that are considered not only to instrumentation errors but also to inherent volume sample variations, the measurements show a trend that the attenuation coefficient slightly decreases as the HEMA content increases from 0 (polymer I) to 25 % (copolymer V) SLS content of about 5 %. The change of the absorption coefficient with variation of SLS and HEMA is a result of the changes of ultrasonic velocities and elastic moduli. This may be related to the decrease in free length  $L_f$  and association of the emulsifier molecules.

The adiabatic compressibility ( $\beta_a$ ), acoustic impedance (Z) and free length ( $L_f$ ) were computed employing the following expressions [17 & 18].

$$\beta_a = V_m^{-2} \rho^{-1} \quad (4)$$

$$Z = \rho V \quad (5)$$

$$L_f = k (\beta)^{1/2} \quad (6)$$

Where,  $V_m$ ,  $\rho$  and  $k$  are respectively, the mean ultrasonic velocity, density for the mixtures and the Jacobson constant ( $0.2 \times 10^{-5} \text{ kg}^{1/2} \text{ m}^{1/2} \text{ s}^{-1}$ ) respectively. The behaviour of  $\beta_a$ , Z and  $L_f$  for all studied samples are displayed in Table 3. The variation of  $\beta_a$  with SLS and HEMA is shown as a typical plot in Figure 7 (a, b). The adiabatic compressibility shows non-linearity with the change in HEMA more than that with the change of SLS, which indicates the possibility of more solute-solvent interaction [25]. Also, the results show significant variations of the acoustic impedance and free length with the variation of SLS and HEMA content. Z and  $L_f$  show the additive molecular behavior in both cases.

For both systems, the measured data of the ultrasonic viscosity is given in Table 3. The data has been compared with that obtained by the dynamic viscosity reasonable agreement has been obtained between the two compared methods As seen in Figure 8 (a, b), they increased with increasing either HEMA or SLS contents in microemulsion samples. This can be ascribed due to the aggregation of HEMA and SLS molecules and the decrease in  $L_f$ .

One can notice some deviation due to the viscosity measured dynamically involving macroscopic displacements in the order of  $\mu\text{m}$ , in which chains repeat as a whole through the network. By comparison, the ultrasonic wave is a small disturbance with typical magnitude in the range of  $\text{\AA}$  that cannot dismantle the molecules; therefore ultrasonic viscosity relates to small-scale mobility of short segments between the mixture molecules [26].

**Table 2: Longitudinal ultrasonic velocity ( $V_l$ ), shear ultrasonic velocity ( $V_s$ ), mean ultrasonic velocity ( $V_m$ ), Young's modulus (GPa), Microhardness (GPa) of MMA/HEMA copolymer having different composition ratios.**

Polymer Code	$V_l$ (m/s)	$V_s$ (m/s)	$V_m$ (m/s)	E (GPa)	H (GPa)
Polymer I	1466	679	765	1.38	0.046
Copolymer II	1481	690	777	1.40	0.047
Copolymer III	1573	752	846	1.56	0.057
Copolymer IV	1575	769	864	1.58	0.061
Copolymer V	1658	845	1005	1.80	0.079
Copolymer VI	1453	665	749	1.35	0.044
Copolymer VII	1568	737	830	1.5	0.052
Copolymer VIII	1600	819	917	1.76	0.079



**Table 3: The ultrasonic absorption coefficient ( $\alpha$ ), ultrasonic viscosity ( $\eta_u$ ), dynamic viscosity ( $\eta_d$ ), adiabatic compressibility ( $\beta_a$ ), acoustic impedance ( $Z$ ) and free length ( $L_f$ ) of MMA/HEMA copolymer having different composition ratios.**

Polymer Code	$\alpha$ (dB/cm)	$\eta_u$ (Pa.s)	$\eta_d$ (Pa.s)	$\beta_a * 10^{-9}$ (s <sup>2</sup> m/kgm)	$Z * 10^2$ (kgm.m <sup>-2</sup> s <sup>-1</sup> )	$L_f$ nm
Polymer I	1.615	37.68	5.31	1.56	8384	78.9
Copolymer II	1.609	38.70	10.1	1.54	8384	78.4
Copolymer III	1.544	45.19	18.12	1.37	8609	74.1
Copolymer IV	1.490	45.35	28.09	1.35	8578	73.5
Copolymer V	1.127	51.76	33.15	1.04	9559	64.5
Copolymer VI	2.000	44.79	6.20	1.59	8386	80.0
Copolymer VII	1.785	49.40	13.13	1.42	8461	75.5
Copolymer VIII	1.593	57.96	28.89	1.20	9092	69.2

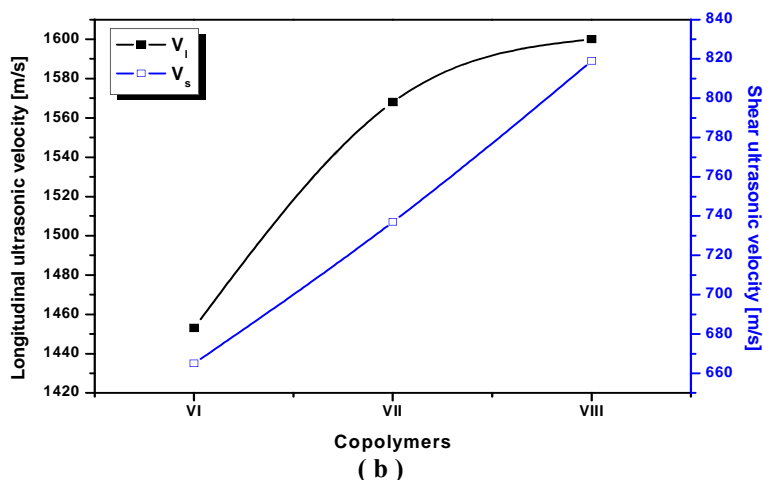
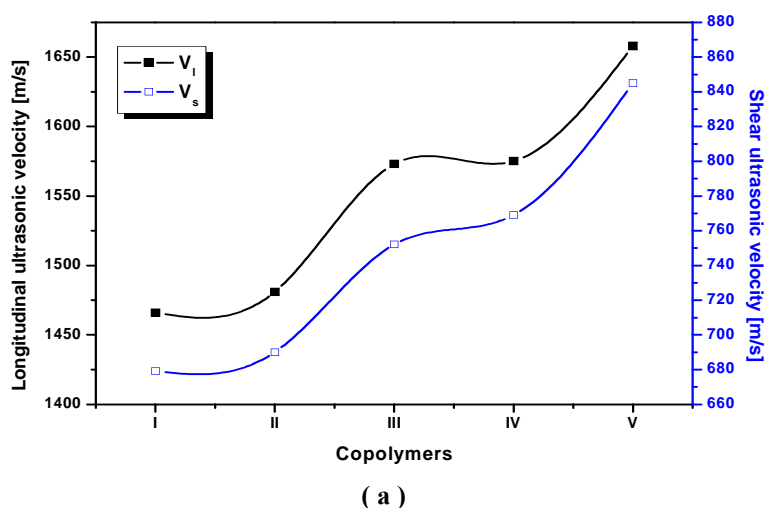
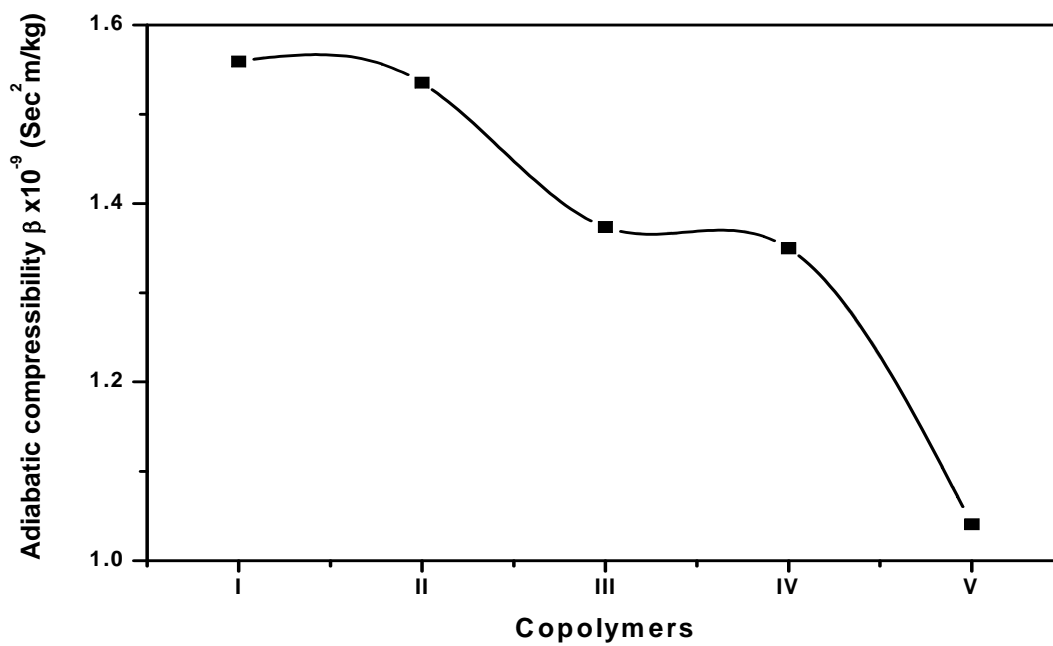
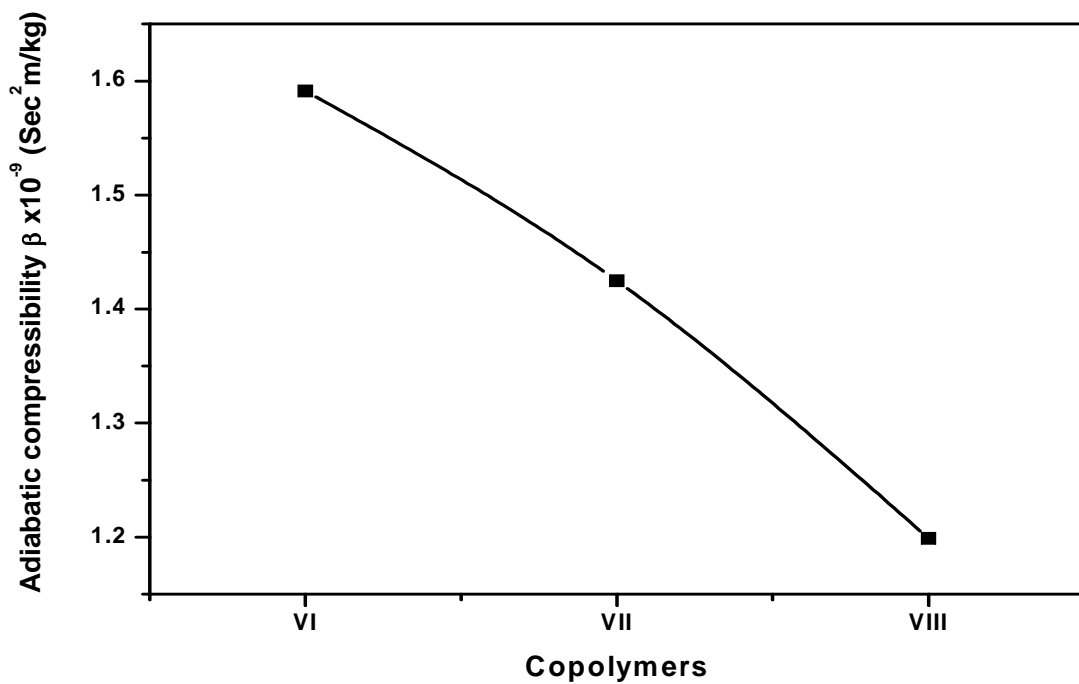


**Figure 6 (a,b): Variation of the longitudinal ultrasonic velocity ( $V_l$ ) and ultrasonic shear velocity ( $V_s$ ) of MMA/BuA copolymers having different composition ratios.**



(a)



(b)

Figure 7 (a,b): Variation of adiabatic compressibility of MMA/BuA copolymers having different composition ratios.

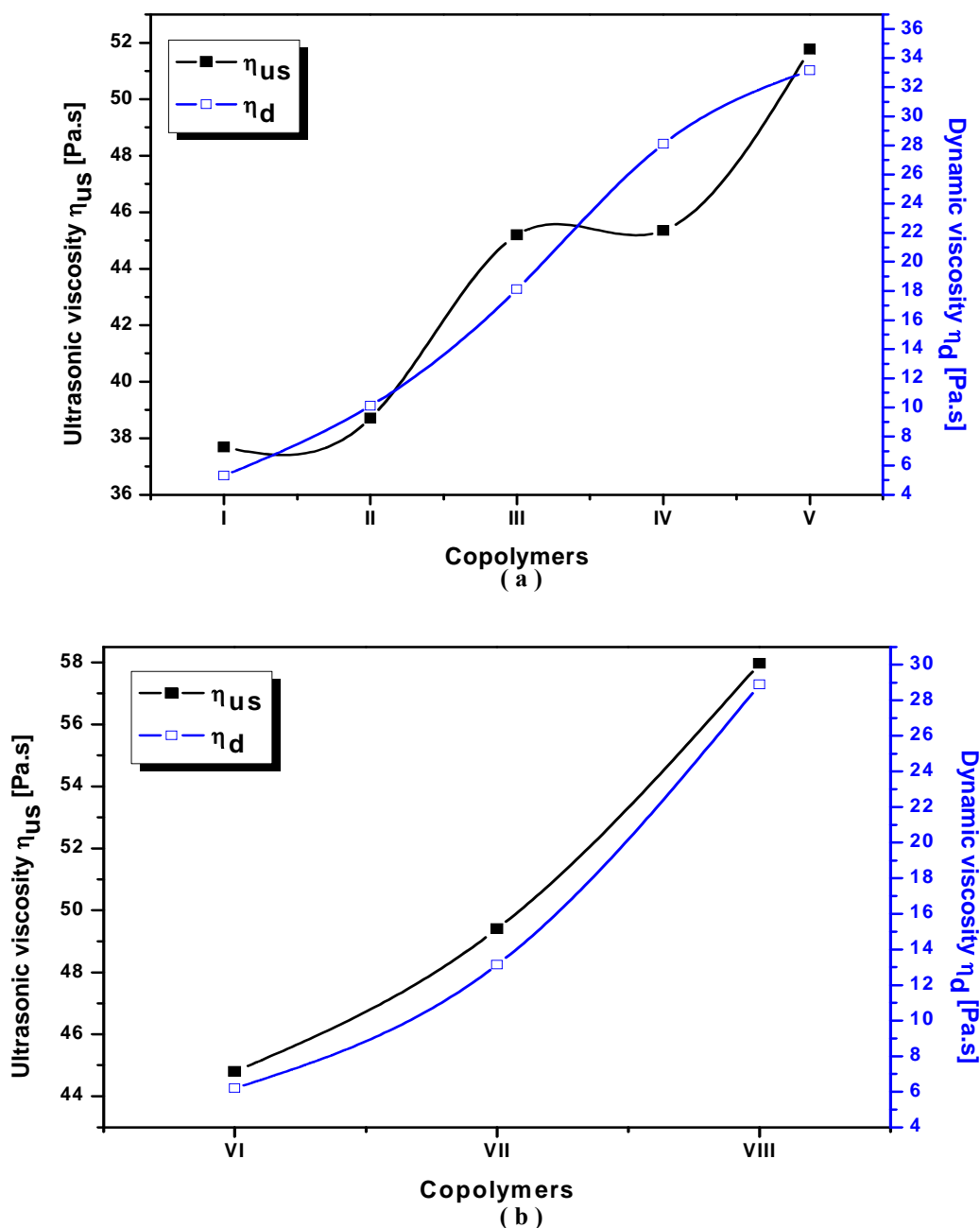


Figure 8 (a,b): Variation of ultrasonic viscosity ( $\eta_u$ ) and dynamic viscosity ( $\eta_d$ ) of MMA/BuA copolymers having different composition ratios.

#### Rheological Characterization

Figures (9-12) show the rheological characterization for microemulsion samples prepared at different MMA/ HEMA monomers composition ratios as well as SLS concentration. From the data shown in Figures (9&10), it is evident that the shear stress is directly proportional to the shear rate for polymer I and copolymer III as well as VI which

clarify Newtonian flow under the condition employed. On the other hand, non - Newtonian, pseudoplastic flows are mentioned for copolymer IV, V and VIII where the curves are convex to shear stress axis. Figures (11&12) show the apparent viscosity of the microemulsion lattices sample as a function of shear rate. There can be noted formation of non Newtonian pseudoplastic viscosity behavior

when the content of HEMA increased over 12.5% in the composition ratio (at 2% SLS) and by increasing SLS concentration up to 5% even at HEMA content ratio of 12.5%. A probable explanation states that, increasing of HEMA content in the feed monomer composition induces an increase of the hydrodynamic volume of particles [27]. Another explanation of this result is the aggregation poly-HEMA which causes formation of pseudoplastic viscosity behavior due to

better orientation of the polymer particles in the direction of rotation at higher shearing rates, thereby offering less resistance to flow [28]. This behavior proved by ultrasonic measurement via decreasing in free length  $L_f$  which is accompanied by increasing either HEMA content ratio or SLS concentration. That is manifesting the explanation of pseudoplastic viscosity behavior by increasing SLS concentration.

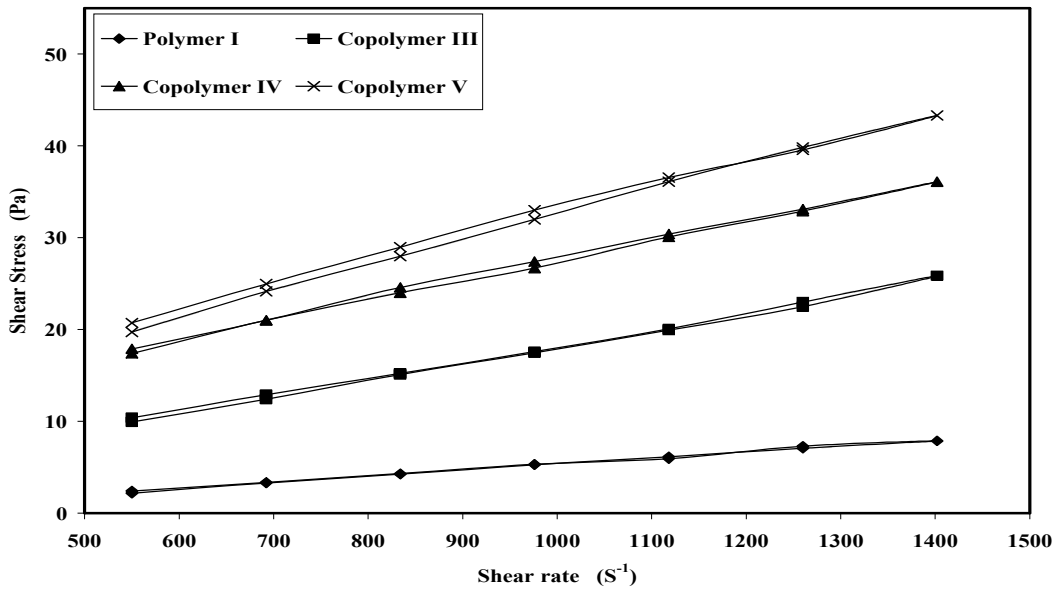


Figure (9): The effect of shear rate on the shear stress of polymer I, polymer III, polymer IV and polymer V.

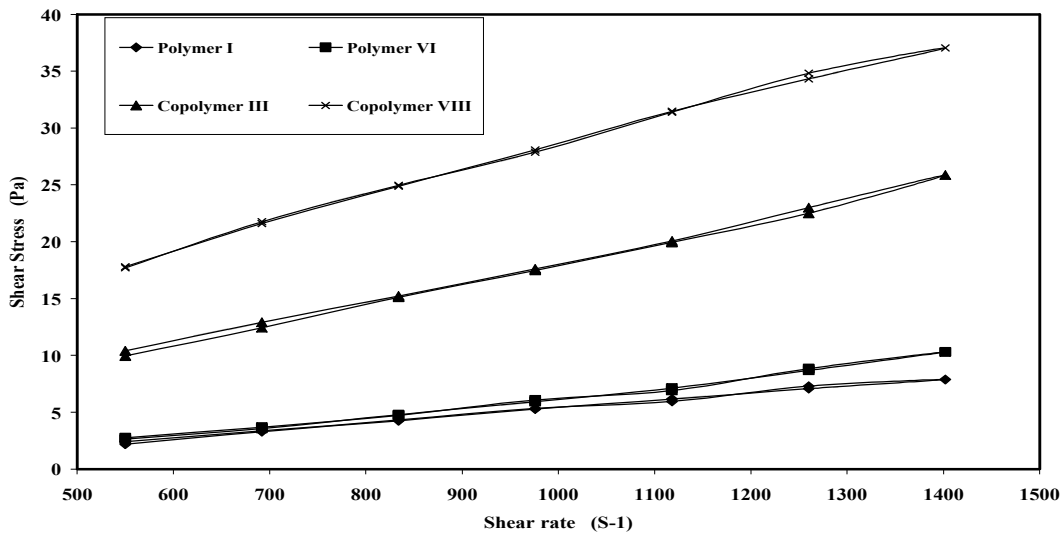


Figure (10): The effect of shear rate on the shear stress of polymer I, polymer III, polymer VI and polymer VIII.

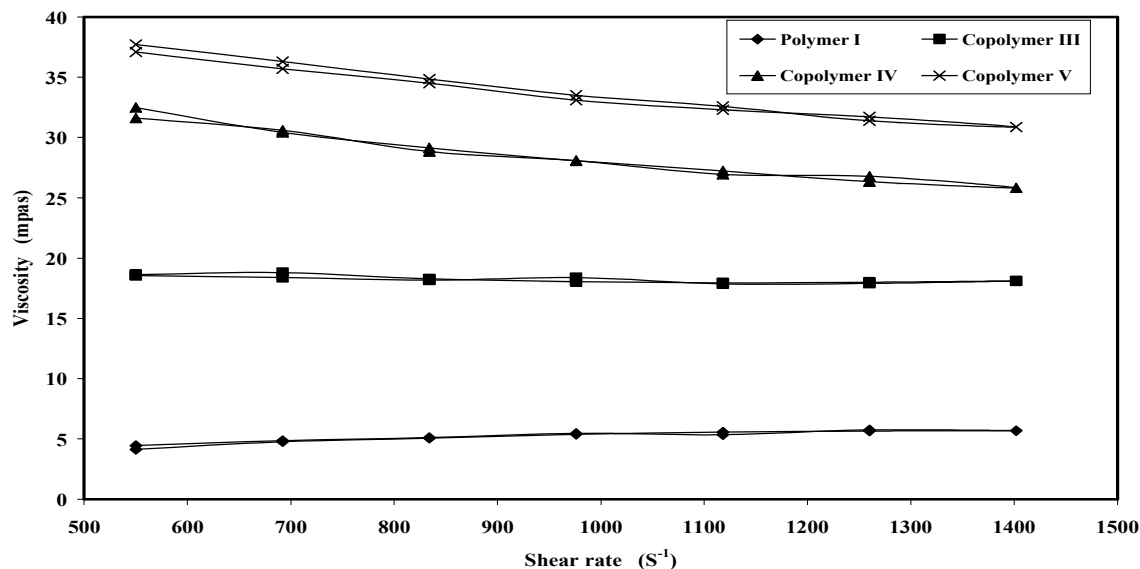


Figure (11): The effect of shear rate on the apparent viscosity of polymer I, polymer III, polymer IV and polymer V.

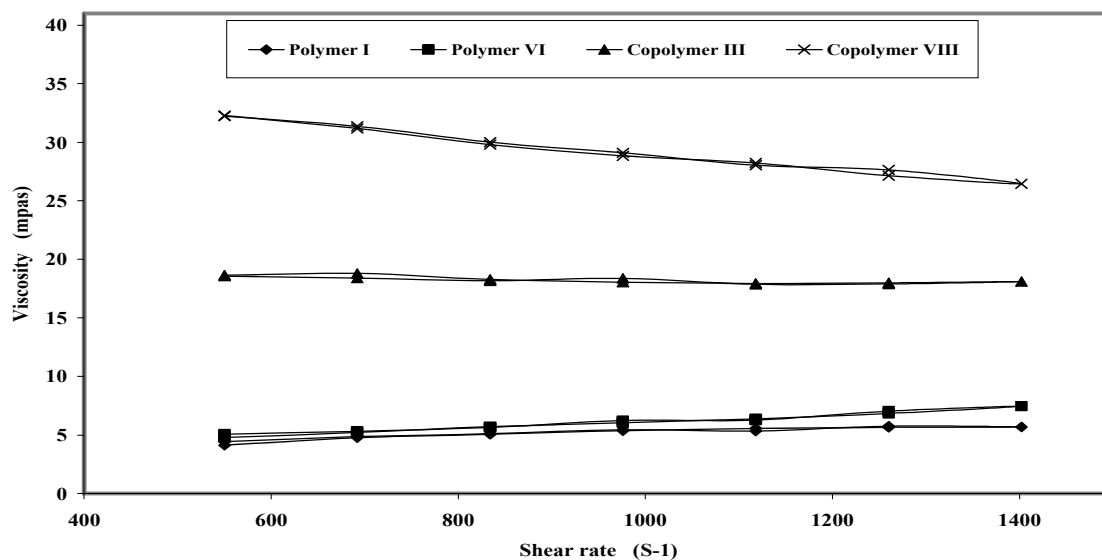


Figure (12): The effect of shear rate on apparent viscosity of polymer I, polymer III, polymer VI and polymer VIII

#### Acknowledgements:

This work has been supported by Science & Technology Development Fund (STDF) through the Project No. 604 entitled "New Strategies for Conservation of Ancient Egyptian Textiles with the Application on Some Selected Textile Objects in the Museum of Faculty of Archaeology, Cairo University"

#### Corresponding author

H. E. Nasr  
<sup>1</sup>Department of Polymers and Pigments National Research Centre, Cairo, Egypt  
[hanaa\\_nasr@hotmail.com](mailto:hanaa_nasr@hotmail.com)

#### 5. References:

1. M. A. Bradley, S. W. Prescott, H. A. S. Schroonbrood and K. Landfester and F. Grieser, *Macromolecules*, 38(15) 6346-6351(2005).

3. B. M. Teo, S. W. Prescott, M. Ashokkumar and F. Grieser, *Ultrason. Sonochem.*, 15(1) 89-94(2008).
4. S. K. Ooi and S. Biggs, *Ultrason. Sonochem.*, 7(3) 125-133(2000).
5. D. J. McClements, *Colloids and Surfaces A: Physicochemical and Engineering Aspects* 90 (1) 25-35 (1994).
6. C. Zhang, Q. Wang, H. Xia and G. Qiu, *European Polymer Journal*, 38 (9) 1769-1776 (2002).
7. L. Yan, J. Ji, D. Xie, W. Li and G. Zhang *Polym. Adv. Technol.*, 19, 221 (2008).
8. Aizpurua, J.I. Amalvy, J.C. de la Cal and M.J. Barandiaran *Polymer*, 42(42) 1417-1427 (2001).
9. M. Li, E.S. Daniels, V. Dimonie, E. D. Sudol, and M.S. El-Aasser. *Macromolecules*, 38(10) 4183-1492 (2005).
10. B.M. Teo, M. Ashokkumar, and F. Grieser. *The Journal of Physical Chemistry Letters*, 112, 5265(2008).
11. G. V. Ramana Reddy, C. Ramesh Kumar and R. Sriram *J Appl Polym Sci.*, 94, 739 (2004).
12. F.D. Karia, P.H. Parsania, *Eur. Polym. J.*, 36 (3) 519 (2000).
13. R.K. Chowdoji, N.S. Venkata and R.A. Varada *Eur. Polym. J.*, 26(6) 657-659(1990).
14. R.A. Varada, R.K. Chowdoji and N. Venkata *Acoustica*, 75, 213-216 (1991).
15. RA Varada and SP Mabu, *J. Polymer Mater*, 12, 87(1995).
16. (15) S. Bhawal, L. H. Reddy, R. S. R. Murthy and S. Devi. *J. Applied Polymer Science*, 92(1) 402-409(2004).
17. F. Özer, M.O. Beskarde, H. Zareie, E. Piskin. *J. of Applied Polymer Science*, 82(1) 237-242(2001).
18. J.H. Kim, Y.M. Lee, *J. Membrane Science*, 193: 209(2001).
19. Y. Mori, R. Saito. *Polymer*, 45: 95-100(2004).
20. M.E. Gaafar, E.A. EL-Sayad and S.Y. Marzouk. *Archives of Acoustics*, 33(3): 363-372(2008).
21. S. Mohanty, G. B. Nando, K. Vijayan and N. R. Neelakanthan. *Polymer*, 37, 5387-5394(1996).
22. P. Sherman, *J. Soc Chem Ind*, 2(Suppl.), 570(1950).
23. P. Sherman, *Kolloid Z*, 165, 156(1959).
24. P. Sherman, *Proc Third Int Congr Surface Activity*, II, 596(1960).
25. Sherman, P. *Food Technol*, 15, 394(1961).
26. S. Srilalitha, M.C. Subha and R.K. Chowdoji. *J. Pure Applied Ultrasonic* 18, 59(1996).
27. M. Mekawy, H. Afifi and Kh. ElNagar, *Comparison between different methods for viscosity Measurements*, 15<sup>th</sup> Symp. For Thermophysical properties, Colorado, USA (NIST), 22-27 June (2003).
28. O. Quadrat, J. Horsky, P. Bradna, J. Snuparek, G.A. Baghaffar. *Progress in Organic Coatings*. 42, 188-193(2001). E.T. Severs, *Rheology of polymer*, Reinhold, New York, p.6(1962)].

8/2/2010